Çukurova Üniversitesi Mühendislik Mimarlık Fakültesi Dergisi, 35(1), ss. 27-38, Mart 2020
Çukurova University Journal of the Faculty of Engineering and Architecture, 35(1), pp. 27-38, March 2020

Non-linear Control of Inverted Pendulum

Serdar COŞKUN[*1]

[1]*Tarsus Üniversitesi, Mühendislik Fakültesi, Makina Mühendisliği Bölümü, Tarsus/Mersin*

Geliş tarihi: 08.11.2019 *Kabul tarihi: 15.05.2020*

Abstract

Presented is a study of non-linear control for an inverted pendulum system. The inverted pendulum system is a great example of an underactuated, non-minimum phase, and highly unstable system. The objective of this research paper is to derive non-linear control laws for an inverted pendulum system. First, dynamic equations of the inverted pendulum are derived by utilizing the Lagrange's equations and then it is linearized around an unstable upright position. Secondly, the corresponding analysis uses the standard linear stability arguments and the traditional Lyapunov method. The non-linear sliding mode control and feedback linearization control laws are then derived The feedback linearization control law is used to transform the non-linear system into an equivalent linear system such that a suitable feedback control law can be proposed. The stabilization of the initial condition and reference tracking is studied in this paper. I demonstrate the effectiveness of the proposed non-linear control strategies using MATLAB/Simulink software.

Keywords: Non-linear control, Inverted pendulum system, Sliding mode control, feedback linearization

Ters Sarkaç Sisteminin Doğrusal Olmayan Kontrolü

Öz

Sunulan bir ters sarkaç sistemi için doğrusal olmayan kontrol çalışmasıdır. Ters sarkaç sistemi eksik tahrikli, karma evreye sahip ve oldukça kararsız bir sistemin en önemli örneğidir. Bu araştırma makalesinin amacı, ters sarkaç sistemi için doğrusal olmayan kontrol yasaları elde etmektir. İlk olarak, ters sarkaçların dinamik denklemleri Lagrange denklemleri kullanılarak türetilir ve daha sonra kararsız dik pozisyon etrafında lineer karalılık noktaları bulunur. Diğer adımda analizler için doğrusal kararlılık teorileri ve Lyapunov metodunu kullanır. Doğrusal olmayan kayan kipli kontrol ve geri beslemeli doğrusallaştırmış kontrol yasaları türetilir. Geri beslemeli doğrusallaştırmış kontrol yasası doğrusal olmayan sistemi eşdeğer bir doğrusal sisteme dönüştürmek için kullanılır, böylece uygun bir geri besleme kontrol yasaları önerilebilir. Başlangıç koşullarından kararlılık ve referans takibi bu makalede incelenmiştir. Önerilen doğrusal olmayan kontrol stratejilerinin kontrol performansı MATLAB/ Simulink programı ile gösterilmiştir.

Anahtar Kelimeler: Linear olmayan kontrol, Sarkaçlı araba sistemi, Kayan kipli kontrol, Geri beslemeli doğrusallaştırılmış kontrol

[*] Sorumlu yazar (Corresponding author): Serdar COŞKUN, *serdarcoskun@tarsus.edu.tr*

1. INTRODUCTION

Recently, the non-linear control theory has received increased attention due to its technical importance and impact on various fields of application. For instance, robotics is one major application for the non-linear control theory. In the robotics control system design, the inverted pendulum is important for modeling. A cart inverted pendulum system has been served as a general model for robotic systems. The cart pendulum system is a non-linear, under-actuated system with unstable zero dynamics and must be controlled such that the position is at its unstable equilibrium [1-5]. The most common method to perform the swing-up of an inverted pendulum is energy control where the energy of the system is controlled instead of directly controlling its position and velocity. As the inverted pendulum deviates from the vertical open-loop unstable position, the proposed control laws make the inverted pendulum a dynamic equilibrium.

Intelligent control methods are proposed in the literature based on non-linear model analysis. A neutral network type learning control method is developed in [6]. The designed control deals with issues of delayed performance evaluation, learning under uncertainty, and the learning of non-linear functions with no prior knowledge of the dynamics. A fuzzy logic control with the Sugeno inference method is used for simultaneous control of the four-state variables including the angular position and the angular velocity of an inverted pendulum, cart position, and cart velocity around unstable equilibrium point as shown in work [7]. The works [8-9] present an optimal tuning of linear quadratic regulator (LQR) controller with the Bees Algorithm (BA) for a linear inverted pendulum system. The Bees Algorithm, which is a heuristic search algorithm, optimizes the weighting matrices of the LQR controller, and results are presented with simulation and experimental studies.

This paper aims to investigate a sliding mode control approach (SMC) and feedback linearization (FL) control approach for an inverted pendulum system and further compare the results. For the controller design view, the paper attempts to perform and compare the sliding mode control and feedback linearization. The sliding mode control is a suitable approach for non-linear control system design [10-12] because it ensures good tracking despite the existence of a parameter uncertainty [13]. According to the switching control law, sliding mode control drives the state trajectory onto the sliding manifold defined by the state variables of the system. However, the switching process often causes a chattering problem for the system. The chattering problem excites undesired flexible dynamics that may cause system instability [14]. To solve this issue, we introduce a saturation function to mitigate the chattering effect while tracking along the sliding surface.

Feedback linearization is another popular method for non-linear control design [15-16]. By introducing a control input to eliminate the non-linear behavior of the system, one can consider the original system as a linear system and further perform linear control such as PID or PD control [17]. However, the drawback of feedback linearization is that it causes the system to behave contrarily to the original system due to its loss of non-linear response.

In this study, the derived control laws are employed to simultaneously balance the inverted pendulum and place the cart via four-state variables, the angular and velocity of the inverted pendulum, and the position and velocity of the cart. Initial condition stabilization and reference tracking performance are both demonstrated. The main contributions of this paper are to find explicit non-linear control laws for stabilization and tracking control of the inverted pendulum system. Results are discussed for the benefits of each technique.

This paper is structured as follows: Section 2 presents the non-linear system modeling of the pendulum-cart system and linearization around the equilibrium position. Section 3 shows nonlinear control methods sliding mode control, and feedback linearization along with the simulation results. Lastly, conclusions are drawn in Section 4.

2. SYSTEM MODELING

In this section, the dynamic model of the pendulum-cart system is derived. With the pin joint connecting the pendulum and the cart, constraint forces are existing in the system, therefore Lagrangian equations are preferred than the Newtonian method.

To apply Lagrangian equations, expressions for the kinetic and potential energies are determined as the cart undergoes translational motion while the pendulum experiences rotational motion. The horizontal displacement of the cart from the pre-defined zero position and the rotational displacement of the pendulum from the upright position. The only actuation in the system is the external force exerted on the cart. The inverted pendulum system has two degrees of freedom. From the geometry (Figure 1), x stands for horizontal displacement of the cart, θ is for the rotation of the pendulum. with M (kg) is the cart mass, m (kg) is the mass of the pendulum, L (m) is the length of the pendulum $g\,(\frac{m}{s^2})$ is the acceleration of gravity. For simplicity, the time dependency on t is omitted. Continous time differential equation is written for the inverted pendulum system in the form of: $\dot{x}=f(x,u)$, where $x \in \mathbb{R}$ is the state vector, $u \in \mathbb{R}$ is the manipulated control input. The parameters of the inverted pendulum are given as follows:

$$M=6 \text{ kg},\ m=2 \text{ kg},\ L=1 \text{ m},\ g=9.81\frac{m}{s^2}$$

We initiate the non-linear modeling of the inverted pendulum system using Lagrangian mechanics. The kinetic energy can be expressed as (Equations 1-3).

$$T=\frac{1}{2}M\dot{x}_c^2+\frac{1}{2}m\left(\dot{x}_p^2+\dot{y}_p^2\right). \tag{1}$$

where

$$x_c = displacement\ of\ cart = x, \tag{2}$$

$$\begin{cases} x_p=\text{horizontal displacement of COM of pendulum}=x+L\sin\theta, \\ y_p=\text{vertical displacement of COM of pendulum}=L\cos\theta, \end{cases} \tag{3}$$

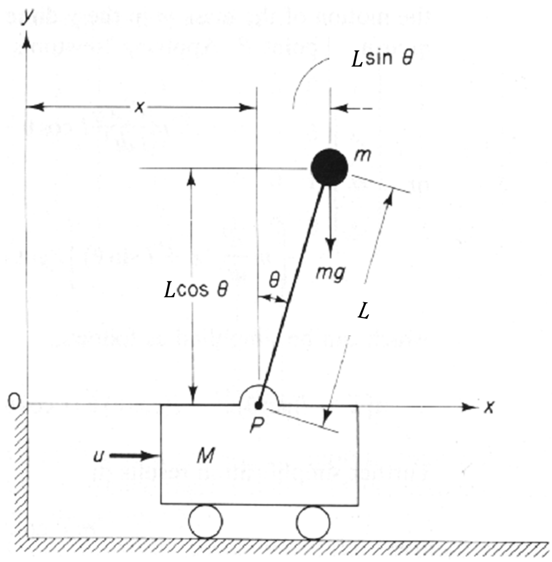

Figure 1. Pendulum-cart system geometry and the corresponding velocities are (Equations 4 and 5).

$$\dot{x}_c = \dot{x}, \tag{4}$$

$$\begin{cases} \dot{x}_p=\dot{x}+L\cos(\theta)\dot{\theta}, \\ \dot{y}_p=-L\sin(\theta)\dot{\theta}, \end{cases} \tag{5}$$

making the kinetic energy as (Equation 6):

$$T=\frac{1}{2}M\dot{x}^2+\frac{1}{2}m\left(\dot{x}^2+L^2\dot{\theta}^2+2L\cos(\theta)\dot{\theta}\dot{x}\right) \tag{6}$$

Meanwhile, the potential energy can be expressed as (Equation 7):

$$V=mgy_p=mgL\cos(\theta) \tag{7}$$

Now the Lagrangian is formulated as follows (Equation 8):

$$\begin{aligned} L=T-V=\frac{1}{2}(M+m)\dot{x}^2+ \\ \frac{1}{2}mL^2\dot{\theta}^2+mL\cos(\theta)\dot{\theta}\dot{x}-mgL\cos(\theta) \end{aligned} \tag{8}$$

After choosing x and θ as the generalized coordinates, the Lagrange's equations become (Equations 9-10):

$$\frac{d}{dt}\left(\frac{\partial L}{\partial \dot{\theta}}\right)-\frac{\partial L}{\partial \theta}=0, \tag{9}$$

$$\frac{d}{dt}\left(\frac{\partial L}{\partial \dot{x}}\right)-\frac{\partial L}{\partial x}=u. \tag{10}$$

Through some algebraic manipulations Equations 9-10, two governing equations of motion are (Equation 11):

$$\begin{cases} ML^2\ddot{\theta}+mL\cos(\theta)\ddot{x}-mgL\sin(\theta)=0, \\ (M+m)\ddot{x}+mL\cos(\theta)\ddot{\theta}-mL\sin(\theta)\dot{\theta}^2=u. \end{cases} \tag{11}$$

or equivalently the following standard form (Equation 12)

$$M(q)\ddot{q}+C(q,\dot{q})\dot{q}+G(q)=f. \tag{12}$$

Where

$$q=\begin{bmatrix}\theta \\ x\end{bmatrix},\ M(q)=\begin{bmatrix} ML^2 & mL\cos(\theta) \\ mL\cos(\theta) & M+m\end{bmatrix},$$

$$C(q,\dot{q})=\begin{bmatrix} 0 & 0 \\ -mL\sin(\theta)\dot{\theta} & 0\end{bmatrix},$$

$$G(q)=\begin{bmatrix} -mgL\sin(\theta) \\ 0\end{bmatrix},\ f=\begin{bmatrix}0 \\ u\end{bmatrix}$$

Notice that the states are coupled and apparently there is only one control in one channel of the actuation vector f, meaning that the system is underactuated and difficult to control. Recall that θ is the pendulum angle, $\dot{\theta}$ is the pendulum angle velocity, x is the cart displacement and $\dot{x}$ is the cart velocity. For the control purpose, four state variables are defined as $(x_1\ x_2\ x_3\ x_4)^T=(\theta\ \dot{\theta}\ x\ \dot{x})^T$ to form the compact non-linear state space equations as follows (Equation 13):

$$\begin{bmatrix}\dot{x}_1 \\ \dot{x}_2 \\ \dot{x}_3 \\ \dot{x}_4\end{bmatrix}=\begin{bmatrix}\dot{\theta} \\ \ddot{\theta} \\ \dot{x} \\ \ddot{x}\end{bmatrix}=\begin{bmatrix} 0 & 1 & 0 & 0 \\ \frac{(M+m)g\sin(\theta)}{\left(M+m\sin^2(\theta)\right)L\theta} & -\frac{m\sin(\theta)\cos(\theta)\dot{\theta}}{M+m\sin^2(\theta)} & 0 & 0 \\ 0 & 0 & 0 & 1 \\ -\frac{mg\cos(\theta)\sin(\theta)}{\left(M+m\sin^2(\theta)\right)\theta} & \frac{mL\sin(\theta)\dot{\theta}}{M+m\sin^2(\theta)} & 0 & 0 \end{bmatrix}\begin{bmatrix}\theta \\ \dot{\theta} \\ x \\ \dot{x}\end{bmatrix}$$

$$+\begin{bmatrix} 0 \\ -\frac{\cos(\theta)}{\left(M+m\sin^2(\theta)\right)L} \\ 0 \\ \frac{1}{M+m\sin^2(\theta)}\end{bmatrix}u \tag{13}$$

2.1. Equilibrium and Stability Analysis

The equilibria points of the cart-pendulum system are obtained to be (Equation 14):

$$\begin{cases} x_{1e}=k\pi, \\ x_{2e}=0, \\ x_{3e}=\alpha, \\ x_{4e}=0. \end{cases} \tag{14}$$

where $k\in\mathbb{Z}$ and $\alpha\in\mathbb{R}$

Even though the system has infinite equilibria mathematically, physically, the equilibria are the upright and the pendant positions of the pendulum with an arbitrary cart displacement. Due to the intended application of the model to robotic system control, the equilibrium of the pendent position (when is an odd number) is not discussed.

To investigate the stability of the equilibria, the Jacobian linearized model around the equilibrium $(0\ 0\ 0\ 0)^T$ is derived directly from the state space equations, which yields, (Equation 15)

$$\dot{x}=Ax+Bu \tag{15}$$

where

$$A=\begin{bmatrix} 0 & 1 & 0 & 0 \\ \frac{(M+m)g}{ML} & 0 & 0 & 0 \\ 0 & 0 & 0 & 1 \\ -\frac{mg}{M} & 0 & 0 & 0 \end{bmatrix},\ B=\begin{bmatrix} 0 \\ -\frac{1}{ML} \\ 0 \\ \frac{1}{M} \end{bmatrix}$$

Since there are two zero eigenvalues and two real eigenvalues with opposite signs, this equilibrium in both the linearized system and the original non-linear system is unstable.

2.2. Performance Analysis

The closed-loop performance of a control system is measured based on a performance index. In this work, we use 3 difference indices for reference tracking error (of the derived SMC and FL control laws. The performance indices are:

1) Integral of the squared value of the error (ISE):

$$ISE=\int_0^\infty e(t)^2\,dt.$$

2) Integral of the absolute value of the error (IAE):

$$IAE=\int_0^\infty \left|e(t)\right|dt.$$

3) Integral of the time-absolute value of the error (ITAE):

$$ITAE=\int_0^\infty t\left|e(t)\right|dt.$$

3. NON-LINEAR CONTROLS AND RESULTS

3.1. Sliding Mode Control

Non-linear systems have inherently been hard to control due to the unexpected responses. The sliding mode controllers have successfully been implemented to the non-linear plant models to achieve the prescribed control and performance objectives. The main idea behind the SMC is that the dynamics of non-linearity is altered by a discontinuous control signal that forces the system to the sliding surfaces. Some of the main advantages of SMC are robustness, faster convergences, and reduced-order controller dynamics. In the scope of this paper, the SMC is capable of controlling the pendulum angle over all operating range. To this end, our design objective is upswing control of the pendulum from the initial condition and to hold the pendulum at a particular angle from the upright position.

The SMC control law is defined as follows:

We first define the dynamics of the pendulum as: (Equations 16-18)

$$\begin{aligned}\dot{x}_1&=x_2,\\ \dot{x}_2&=h(x)+g(x)u.\end{aligned} \tag{16}$$

where

$$h(x)=\frac{(M+m)g\sin(\theta)-mL\sin(\theta)\cos(\theta)\dot{\theta}^2}{\left(M+m\sin^2(\theta)\right)L}, \tag{17}$$

$$g(x)=-\frac{\cos(\theta)}{\left(M+m\sin^2(\theta)\right)L} \tag{18}$$

A sliding surface for the non-linear system is given (Equation 19)

$$s=\lambda x_1+x_2 \tag{19}$$

λ denotes the distance of the state from the sliding surface. In our design, λ is selected to be 3. Assume the corresponding positive definite Lyapunov function with a negative definite derivative along the system trajectories (Equations 20 and 21)

$$V=\frac{1}{2}s^2 \tag{20}$$

$$\dot{V}=s\dot{s}=s\left(\lambda\dot{x}_1+\dot{x}_2\right)=s\left(\lambda x_2+h(x)+g(x)u\right)<0 \tag{21}$$

Then we define the non-linear control law that is applied to the system (Equation 22):

$$u(t)=\frac{1}{g(x)}\left(-\lambda x_2-h(x)\right)-K\mathrm{sign}\left(\lambda x_1+x_2\right) \tag{22}$$

Further arrangements led to (Equation 23)

$$u=-\frac{\left(M+m\sin^2(\theta)\right)L}{\cos(\theta)}\left(-\lambda\dot{\theta}-\frac{(M+m)g\sin(\theta)-mL\sin(\theta)\cos(\theta)\dot{\theta}^2}{\left(M+m\sin^2(\theta)\right)L}\right)-K\mathrm{sign}\left(\lambda\theta+\dot{\theta}\right). \tag{23}$$

Note that we design the control law only for the pendulum angle and velocity. This control law guarantees the upward position and stabilization of the pendulum. However, it has no effects on the cart position and velocity. Therefore, another sliding mode control law, using a sliding surface $s=\beta x_1+x_2$ and repeating the computations in Equations 20-22, is found and applied to the cart (Equation 24)

$$u=\left(M+m\sin^2(\theta)\right)\left(-\beta x+\frac{mg\cos(\theta)\sin(\theta)-mL\sin(\theta)\dot{\theta}^2}{M+m\sin^2(\theta)}\right)-K\mathrm{sign}\left(\beta x+\dot{x}\right) \tag{24}$$

where β is chosen as 5. λ and β can be realized as sliding surface convergence speed and the best running performance is observed with the selected values. To verify and compare the performance of the proposed control law, the inverted pendulum simulation system is built in MATLAB/Simulink. The first design purpose is to stabilize the pendulum at upward position for a given initial condition. We chose the initial pendulum angle as $0.2*\pi=(36°)$ and let the system reach the equilibrium position.

It is obvious that the designed control drives the system to the equilibrium within a reasonable amount of time ($3\ secs$) in Figure 2 and Figure 3. The notorious problem with this control is that the chattering in the control input. This because the switching control law depends on the system state value, which strives to drive the states to the sliding surface that can never reach to the surface exactly. It is quite harmful to the mechanical systems. Figure 4 demonstrates the situation.

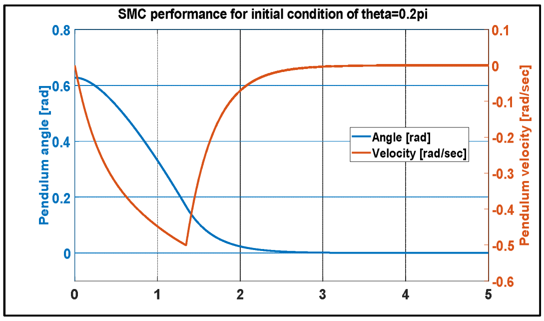

Figure 2. Stabilization of pendulum angle and velocity

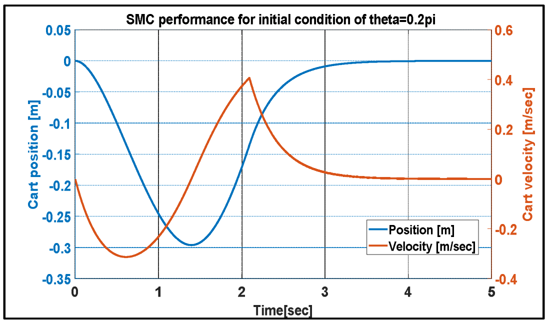

Figure 3. Stabilization of cart position and velocity

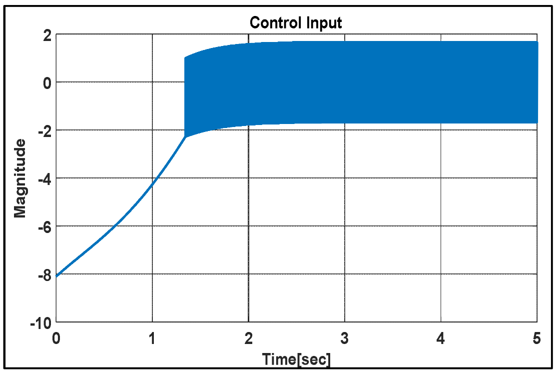

Figure 4. Control input

The performance measures of this control law in reference tracking (Figure 10) are stated as follows: the integral squared error (ISE) is 8.194, integral absolute error (IAE) is 4.91, and the integral time-absolute error (ITAE) is 17.13.

One way of eliminating this undesired behavior of the control input is to introduce a tolerance band, ε,(saturation function) around the sliding surface. When ε=0.7, the following figures demonstrate the results.

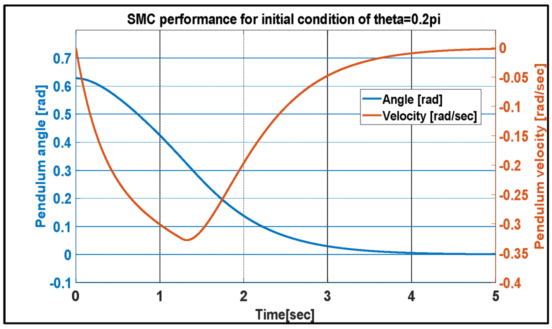

Figure 5. Stabilization of pendulum angle and velocity with ε=0.7

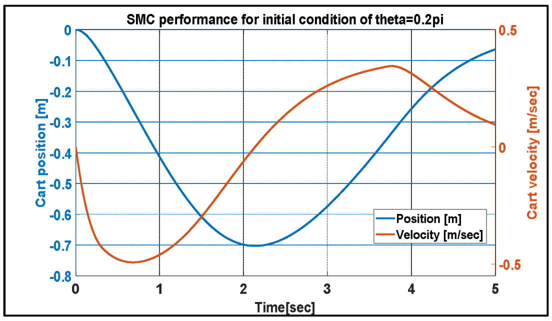

Figure 6. Stabilization of cart position and velocity ε=0.7

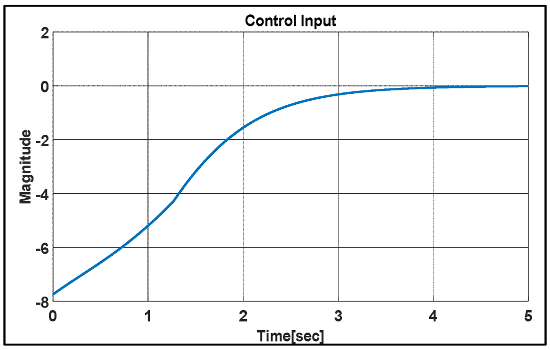

Figure 7. Control input ε=0.7

It is explicitly shown that the chattering effect on the control input is successfully eliminated. However, the settling time has increased in Figures 5 and 6. It is seen that there is always a trade-off on the control design in Figure 7.

For the sake of demonstration, we also plot the phase plane portraits of the non-linear system with and without saturation function.

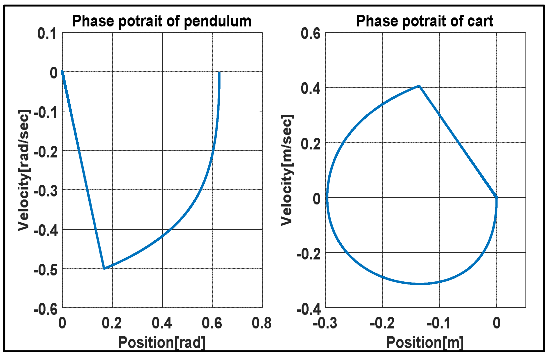

Figure 8. Phase portraits of SMC

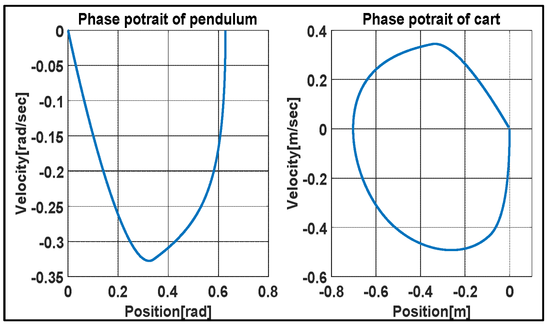

Figure 9. Phase portraits of SMC with ε=0.7

Figure 8 shows the improved convergence of the position and velocity for the pendulum and cart with a sharp path. However, Figure 9 has softer convergence map over the trajectories.

We now go further and test the designed controller for a given position of the pendulum. We set the angle θ=0.095*π=0.3 (17.2°). At 2 seconds the pendulum position is set to 17.2°. We avoid having a sharp reference following. It takes 2 seconds for the pendulum to settle at the desired position in Figure 10. Chattering effect of the controller is displayed in the same figure as well.

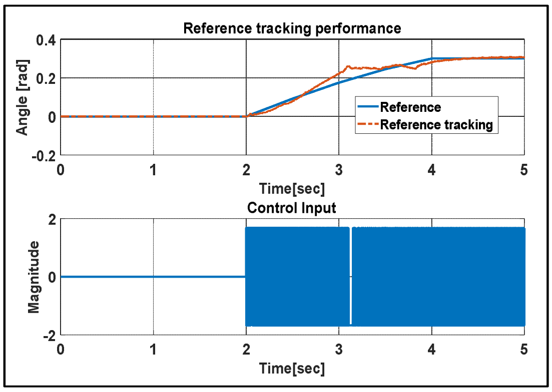

Figure 10. Constant reference tracking of SMC

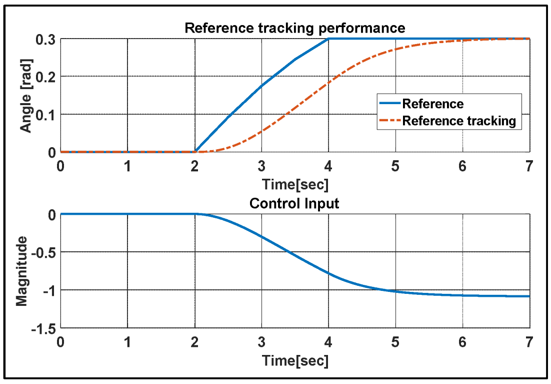

Figure 11. Constant reference tracking of SMC $\varepsilon = 0.7$

The tracking performance of controller with a saturation tolerance of ε=0.7 is also tested. As expected, small deviation occurs around the set position of the pendulum. The controller achieves to balance the pendulum at the desired position in a longer time period, seen in Figure 11.

The performance measures of SMC with $\varepsilon = 0.7$ are stated as follows: the integral squared error (ISE) is 0.0009469, integral absolute error (IAE) is 0.05336, and the integral time-absolute error (ITAE) is 0.1986.

3.2. Feedback Linearization Control

Feedback linearization (FL) control transforms a non-linear system dynamics into a linear dynamics so that the linear control methods can be applied. We employ the input-output linearization for the non-linear plant. We first derive the input to the pendulum angle feedback linearization, the pendulum displacement is considered as output. The control objective is to regulate the pendulum at the upright position. It is seen that the internal dynamics of the system is unstable. Even though the input to the pendulum angle control law stabilizes the pendulum position in an upright direction, it has no control for the displacement of the cart. In the upcoming steps, we also derive the input to the cart displacement control law to be able to regulate the entire closed-loop dynamics. We first write down the system Equations 25-28:

$$\dot{x}=f(x)+g(x)u \tag{25}$$

$$y=h(x) \tag{26}$$

where

$$f(x)=\begin{bmatrix} \dot{\theta} \\ \dfrac{(M+m)g\sin(\theta)-mL\sin(\theta)\cos(\theta)\dot{\theta}}{\left(M+m\sin^2(\theta)\right)L} \\ \dot{x} \\ \dfrac{-mg\cos(\theta)\sin(\theta)+mL\sin(\theta)\dot{\theta}}{M+m\sin^2(\theta)} \end{bmatrix} \tag{27}$$

$$g(x)=\begin{bmatrix} 0 \\ -\dfrac{\cos(\theta)}{\left(M+m\sin^2(\theta)\right)L} \\ 0 \\ \dfrac{1}{M+m\sin^2(\theta)} \end{bmatrix} \tag{28}$$

3.2.1. Lie Derivative

Consider a scalar function $h: D \subset R^n \rightarrow R$ and define a vector field $f: D \subset R^n \rightarrow R$. The Lie derivative of h with respect to f, denoted $L_f h$, is given by

$$L_f h(x)=\frac{\partial h}{\partial x} f(x)$$

And the output is chosen to be the angular displacement of the pendulum (Equation 29):

$$h(x) = x_1 = \begin{bmatrix} 1 & 0 & 0 & 0 \end{bmatrix} \begin{bmatrix} x_1 \\ x_2 \\ x_3 \\ x_4 \end{bmatrix} \tag{29}$$

Then, we can now take the Lie derivate of the output function until the control input appears (Equation 30):

$$\dot{\mathrm{h}} = \frac{\partial h}{\partial x}\dot{\mathrm{x}} = \mathrm{L_f h + L_g hu} = \begin{bmatrix} 1 & 0 & 0 & 0 \end{bmatrix}\left[\mathrm{f}(\mathrm{x})\right] + \begin{bmatrix} 1 & 0 & 0 & 0 \end{bmatrix}\left[\mathrm{g}(\mathrm{x})\right]\mathrm{u} = \mathrm{x_2}, \tag{30}$$

Taking the second derivative in subsequent step results in (Equations 31 and 32):

$$\ddot{\mathrm{h}} = \frac{\partial \dot{h}}{\partial x}\dot{\mathrm{x}} = \mathrm{L_f}^2\mathrm{h} + \mathrm{L_f L_g hu} = \begin{bmatrix} 0 & 1 & 0 & 0 \end{bmatrix}\left[f(x)\right] + \begin{bmatrix} 0 & 1 & 0 & 0 \end{bmatrix}\left[\mathrm{g}(\mathrm{x})\right]\mathrm{u}. \tag{31}$$

$$\ddot{\mathrm{h}} = \ddot{\theta} = \frac{(\mathrm{M+m})\mathrm{g}\sin(\theta) - \mathrm{mL}\sin(\theta)\cos(\theta)\dot{\theta}^2}{\left(\mathrm{M+m}\sin^2(\theta)\right)\mathrm{L}} - \frac{\cos(\theta)}{\left(\mathrm{M+m}\sin^2(\theta)\right)\mathrm{L}}\mathrm{u}. \tag{32}$$

The linearizing control law is chosen as (Equations 33 and 34):

$$\mathrm{u} = \frac{1}{\mathrm{L_f L_g h}}\left(-\mathrm{L_f}^2\mathrm{h} + \mathrm{v}\right), \tag{33}$$

$$\mathrm{u} = -\frac{\left(\mathrm{M+m}\sin^2(\theta)\right)\mathrm{L}}{\cos(\theta)}\left(\frac{-(\mathrm{M+m})\mathrm{g}\sin(\theta) + \mathrm{mL}\sin(\theta)\cos(\theta)\dot{\theta}^2}{\left(\mathrm{M+m}\sin^2(\theta)\right)\mathrm{L}} + \mathrm{v}\right) \tag{34}$$

v is being the new control input variable and can be chosen as $\mathrm{v} = \begin{bmatrix} \mathrm{K_1} & \mathrm{K_2} \end{bmatrix}\begin{bmatrix} \mathrm{x_1} \\ \mathrm{x_2} \end{bmatrix}$ with $\mathrm{K_1} = \mathrm{K_2} = 20$ in our control design. The relative degree is 2. When the the output is chosen to be the cart displacement we have (Equation 35):

$$\mathrm{h}(\mathrm{x}) = \mathrm{x_3} = \begin{bmatrix} 0 & 0 & 1 & 0 \end{bmatrix}\begin{bmatrix} \mathrm{x_1} \\ \mathrm{x_2} \\ \mathrm{x_3} \\ \mathrm{x_4} \end{bmatrix} \tag{35}$$

We take the Lie derivate of the output function one more time until the control input appears (Equation 36):

$$\dot{\mathrm{h}} = \frac{\partial h}{\partial x}\dot{\mathrm{x}} = \mathrm{L_f h + L_g hu} = \begin{bmatrix} 0 & 0 & 1 & 0 \end{bmatrix}\left[\mathrm{f}(\mathrm{x})\right] + \begin{bmatrix} 0 & 0 & 1 & 0 \end{bmatrix}\left[\mathrm{g}(\mathrm{x})\right]\mathrm{u} = \mathrm{x_4} \tag{36}$$

Taking the second derivative leads to (Equations 37 and 38):

$$\ddot{\mathrm{h}} = \frac{\partial \dot{h}}{\partial x}\dot{\mathrm{x}} = \mathrm{L_f}^2\mathrm{h} + \mathrm{L_f L_g hu} = \begin{bmatrix} 0 & 0 & 0 & 1 \end{bmatrix}\left[\mathrm{f}(\mathrm{x})\right] + \begin{bmatrix} 0 & 0 & 0 & 1 \end{bmatrix}\left[\mathrm{g}(\mathrm{x})\right]\mathrm{u}. \tag{37}$$

$$\ddot{\mathrm{h}} = \ddot{\mathrm{x}} = \frac{-\mathrm{mg}\cos(\theta)\sin(\theta) + \mathrm{mL}\sin(\theta)\dot{\theta}^2}{\mathrm{M+m}\sin^2(\theta)} + \frac{1}{\mathrm{M+m}\sin^2(\theta)}\mathrm{u} \tag{38}$$

The linearizing control law is chosen as (Equations 39 and 40):

$$\mathrm{u} = \frac{1}{\mathrm{L_f L_g h}}\left(-\mathrm{L_f}^2\mathrm{h} + \mathrm{v}\right) \tag{39}$$

$$\mathrm{u} = \left(\mathrm{M+m}\sin^2(\theta)\right)\left(\frac{\mathrm{mg}\cos(\theta)\sin(\theta) - \mathrm{mL}\sin(\theta)\dot{\theta}^2}{\mathrm{M+m}\sin^2(\theta)} + \mathrm{v}\right) \tag{40}$$

with $v = \begin{bmatrix} K_3 & K_4 \end{bmatrix} \begin{bmatrix} x_3 \\ x_4 \end{bmatrix}$ with $K_3 = K_4 = 20$ in our control design. Our design objective with the feedback linearization control laws is upswing control of the pendulum from the initial condition and to hold the pendulum at a particular angle from the upright position.

Note that we use same inital condition for the pendulum angle $(0.2 * \pi)$. The results are shown in Figures 12-14.

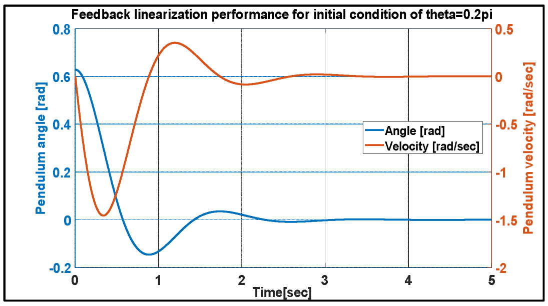

Figure 12. FL stabilization of pendulum angle and velocity

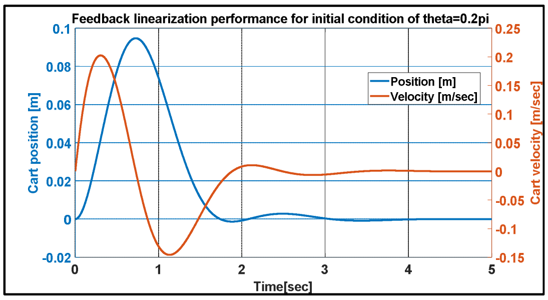

Figure 13. FL stabilization of cart displacement and velocity

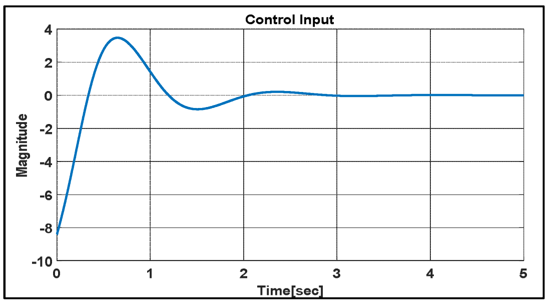

Figure 14. FL control input

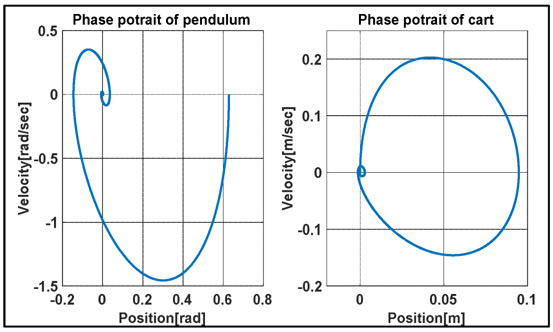

Figure 15. Phase portraits of FL control

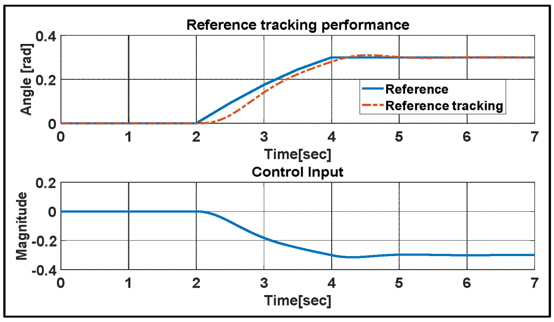

Figure 16. Constant reference tracking and control input of FL control

We make observations on how the states evolve differently than the ones in sliding mode control. Using high control gains for the FL controlled case, we see an overshoot on the control input but fast convergence of the states from the initial conditions (Figures 12 and 13). There is always a trade-off between the desired performance vs. the control action the control design step, illustrated in Figure 14. Phase portraits of the pendulum-cart are shown in Figure 15. Next, we provide a reference angle (17.2°) at 2 seconds and let the controller follow the reference angle within 2 seconds in Figure 16. Even though there is a deviation along the trajectory, the control does an appealing job. The feedback linearization control law closed-loop system performance can also be measured in terms of performance indices. The performance measures are stated as follows: the integral squared error (ISE) is 0.0004306, integral absolute error (IAE) is 0.03057, and the integral time-absolute error (ITAE) is 0.1016. As observed, the best performance is attained with the derived feedback linearization control law for the pendulum-cart system.

4. CONCLUSION

Non-linear control of an inverted pendulum-cart system is presented in this paper. Firstly, the derivation of non-linear differential equations with the stability analysis of equilibrium positions is carried out. Then, two control methods are proposed for the problem. The first one is sliding mode control, which indeed performs a good stabilization and trajectory tracking as expected. One drawback of the SMC is the chattering effect, for which a saturation tolerance is proposed to eliminate the negative impacts on the control input. The second approach is the feedback linearization method that nicely transforms the non-linear system into a linear one, making all types of linear control techniques feasible. It has been demonstrated that the designed non-linear controllers are successfully implemented and the results obtained are quite satisfactory.

5. REFERENCES

1. Chanchareon, R., Sangveraphunsiri, V., Chantranuwathana, S., 2006. Tracking Control of an Inverted Pendulum Using Computed Feedback Linearization Technique. In 2006 IEEE Conference on Robotics, Automation and Mechatronics 1-6, IEEE.
2. Du, L., Cao, F., 2015. Nonlinear Controller Design of the Inverted Pendulum System based on Extended State Observer. In 2015 International Conference on Automation, Mechanical Control and Computational Engineering. Atlantis Press.
3. Zare, A., Lotfi, T., Gordan, H., Dastranj, M., 2012. Robust Control of Inverted Pendulum Using Fuzzy Sliding Mode Control and Particle Swarm Optimization Pso Algorithm. International Journal of Scientific & Engineering Research, 3(10), 1-5.
4. Brisilla, R.M., Sankaranarayanan, V., 2015. Nonlinear Control of Mobile Inverted Pendulum. Robotics and Autonomous Systems, 70, 145-155.
5. Stellet, J. Control of an Inverted Pendulum
6. Anderson, C.W., 1989. Learning to Control an Inverted Pendulum Using Neural Networks. IEEE Control Systems Magazine, 9(3), 31-37.
7. Gani, A., Kececioglu, O.F., Acikgoz, H., Sekkeli, M., 2017. Fuzzy Logic Controller Design Based on Sugeno Inference Method for Nonlinear Inverted Pendulum Dynamical System. Sigma Journal of Engineering and Natural Sciences-Sigma Muhendislik ve Fen Bilimleri Dergisi, 8(1), 19-30.
8. Şen, M.A., Bilgiç, H.H., Kalyoncu, M., 2016. Çift Ters Sarkaç Sisteminin Denge ve Konum Kontrolü için Arı Algoritması ile Lqr Kontrolcü Parametrelerinin Tayini. Mühendis ve Makina, 57(679), 53-62.
9. Bilgic, H.H., Sen, M.A., Kalyoncu, M., 2016. Tuning of LQR Controller for an Experimental Inverted Pendulum System Based on the Bees Algorithm. Journal of Vibroengineering, 18(6), 3684-3694.
10. Köse, E., Abaci, K., Kizmaz, H., Aksoy, S., Yalçin, M.A., 2013. Sliding Mode Control Based on Genetic Algorithm for WSCC Systems Include of SVC. Elektronika ir Elektrotechnika, 19(4), 25-28.
11. Köse, E., 2017. Controller Design by Using Non-linear Control Methods for Satellite Chaotic System. Electrical Engineering, 99(2), 763-773.
12. Irfan, S., Mehmood, A., Razzaq, M.T., Iqbal, J. 2018. Advanced Sliding Mode Control Techniques for Inverted Pendulum: Modelling and Simulation. Engineering Science and Technology, an International Journal, 21(4), 753-759.
13. Grossimon, P., Barbieri, E., Drakunov, S., 1996. Sliding Mode Control of an Inverted Pendulum, System Theory, Proceedings of the Twenty-Eighth Southeastern Symposium, ISBN 0-8186-7352-4, pp.248-252, 31 Mar - 02 Apr 1996 IEEE.
14. Naik, M., Cochran, D., 2012. System Identification of an Inverted Pendulum ona Cart using Compressed Sensing, Signals, Systems and Computers (ASILOMAR), 2012 Conference Record of the Forth Sixth Asilomar Conference, pp.426-430, 4-7 Nov 2012 IEEE.

15. de Jesús Rubio, J., 2018. Robust Feedback Linearization for Nonlinear Processes Control. ISA Transactions, 74, 155-164.

16. Moreno-Valenzuela, J., Aguilar-Avelar, C., 2018. Feedback Linearization Control of the IWP. In Motion Control of Underactuated Mechanical Systems, 141-158, Springer, Cham.

17. Bugeja, M., 2003. Non-linear Swing-up and Stabilizing Control of an Inverted Pendulum System. In The IEEE Region 8 EUROCON 2003. Computer as a Tool. 2, 437-441, IEEE.